Wind and Structures, *Vol. 22, No. 4 (2016) 455-476*
DOI: http://dx.doi.org/10.12989/was.2016.22.4.455

Wind direction field under the influence of topography, part I: A descriptive model

A.U. Weerasuriya[1], Z.Z. Hu[2], S.W. Li[*3] and K.T. Tse[1]

[1]*Department of Civil and Environmental Engineering, Hong Kong University of Science and Technology, Clear Water Bay, Kowloon, Hong Kong*
[2]*Department of Civil Engineering, Tsinghua University and Graduate School at Shenzhen, Tsinghua University, P.R. China*
[3]*Division of Ocean Science and Technology, Graduate School at Shenzhen, Tsinghua University, Shenzhen, P.R. China*

(Received July 17, 2015, Revised January 18, 2016, Accepted February 8, 2016)

Abstract. In both structural and environmental wind engineering, the vertical variation of wind direction is important as it impacts both the torsional response of the high-rise building and the pedestrian level wind environment. In order to systematically investigate the vertical variation of wind directions (i.e., the so-called 'twist effect') induced by hills with idealized geometries, a series of wind-tunnel tests was conducted. The length-to-width aspect ratios of the hill models were $1/3$, $1/2$, 1, 2 and 3, and the measurements of both wind speeds and directions were taken on a three-dimensional grid system. From the wind-tunnel tests, it has been found that the direction changes and most prominent at the half height of the hill. On the other hand, the characteristic length of the direction change, has been found to increase when moving from the windward zone into the wake. Based on the wind-tunnel measurements, a descriptive model is proposed to calculate both the horizontal and vertical variations of wind directions. Preliminarily validated against the wind-tunnel measurements, the proposed model has been found to be acceptable to describe the direction changes induced by an idealized hill with an aspect ratio close to 1. For the hills with aspect ratios less than 1, while the description of the vertical variation is still valid, the horizontal description proposed by the model has been found unfit.

Keywords: descriptive model; hill terrain; wind characteristics; wind-tunnel test

1. Introduction

A reliable and accurate model describing the wind field perturbed by three dimensional hills is of great importance in various fields. For example, a model calculating the vertical profiles of mean wind speeds and directions at the site of interest is useful in assessing wind loads acting on buildings constructed in a mountainous area. Furthermore, studies of air pollution dispersions in mountainous areas may utilize the model to predict the impact of hilly topographies on air pollutants transportations and dispersions (Jazcilevich *et al*. 2005). In addition, an assessment of inland wind energy resource relies heavily on wind resource assessment model such as WAsP

*Corresponding author, E-mail: li.sunwei@sz.tsinghua.edu.cn

Copyright © 2016 Techno-Press, Ltd.
http://www.techno-press.org/?journal=was&subpage=8 ISSN: 1226-6116 (Print), 1598-6225 (Online)

(Wind Atlas Analysis and Application Program)* to determine if a location of interest, which is on the complex and hilly topography, is suitable for wind energy productions (Palma *et al*. 2008).

Given the importance of modelling the wind field perturbed by hilly terrains, wind flows over idealized hills have been studied for several decades, and a number of theoretical models have been proposed to describe the influence of hills on the mean wind speed field (the speed-up effect) and on the turbulence field. For example, Jackson and Hunt (1975) developed the internal boundary layer theory to describe the wind field perturbed by a low hill. The internal boundary layer theory divides the wind field into the inner and outer layers, and the hill was assumed to primarily influence the inner layer flow. Taylor and Lee (1984) followed the theory and suggested guidelines for estimating both horizontal and vertical wind speed variations in the wind field perturbed by small-scale topographic features. In addition, the linear theory presented by Jackson and Hunt (1975) for perturbations induced by a two dimensional low hill was extended by Mason and Sykes (1979) to describe perturbations due to a three dimensional hill with moderate slopes. The model proposed by Mason and Sykes (1979) formed the basis for developing a series of even more sophisticated models. In particular, Taylor *et al*. (1983) introduced the description of terrain in the wavenumber space which helps apply the theory of Mason and Sykes (1979) to wind flows above real, complex terrain.

It should be pointed out that the previously mentioned models are principally used to describe the influence on the mean wind speed field over terrains (the speed-up effect). The influence on the wind direction field, which is equally important, has rarely been the topic of previous studies. To facilitate the discussion, the influence on the wind direction field would be referred to as “twist effect” hereafter, and the yaw angle of a wind velocity vector, which is defined as the angle between the lateral and the longitudinal wind velocities, i.e.

$$\theta = \tan\frac{v}{u} \tag{1}$$

is introduced. In Eq. (1), v is the lateral wind velocity and u is the longitudinal wind velocity. It should be noted that the definitions of longitudinal and lateral directions are based on the approaching wind flow rather than the orientation of the hill. Because it is evident that the vertical variation of yaw angles impacts the torsional response of tall buildings, the need to study the twist effect is justified from a structural wind engineering perspective. More importantly, since the interactions between the approaching wind flow and the building cluster are certainly different in a straight wind flow, in which the yaw angle remains constant vertically, and in a twisted wind flow, it is of practical importance, in terms of assessing the pedestrian level wind field in an urban area, to investigate the change of direction. Given the importance and potential impacts of the twisting effect, it is necessary to develop an engineering-applicable model concerning the direction changes induced by hills with idealized geometries.

While many models are available to depict the speed-up effect, the model describing the twist effect has been rarely investigated. The study of Gong and Ibbetson (1989) and the model suggested by Engineering Science Data Unit (ESDU 1993) are the only published works concerning the twist effect that the authors are aware of. Gong and Ibbetson (1989) investigated the flow patterns around an idealized hill model, which included wind direction perturbations. The investigation of the wind direction field was, however, not the main focus in their study but only used to explain the speed-up effect observed at upwind and downwind sides of the hill.

* http://www.wasp.dk/

Although the ESDU model calculates the three-dimensional variations of yaw angles, it has, to the authors' best knowledge, never been scientifically validated using either the field measurements or the wind-tunnel test results. More importantly, the ESDU model does not make full use of the information provided by the mean wind speed field above the terrain. In the wind field perturbed by a three dimensional hill, it is apparent that wind direction perturbations are physically related to the perturbations in the wind speed field. Consequently, it is an advantage, for a descriptive model of direction changes, to use reliable wind speed estimates derived from a model of the speed-up effect.

Since (a) the twist effect is important from the perspectives of both structural and environmental wind engineering and (b) the ESDU model, which is the only engineering model describing the twist effect, has not yet been scientifically validated, it is necessary to systematically investigate the twist effect in a controlled environment. Therefore, a series of wind-tunnel experiments was conducted to reveal the wind direction field perturbed by a number of low hill models with different length-to-width aspect ratios. From the wind-tunnel measurements, the vertical and horizontal variations of the yaw angles were calculated. Examining the variations leads to the proposition of a descriptive model. Through comparison of the model predictions to the wind-tunnel measurements, the proposed model is preliminarily validated. While the present paper validates the proposed model based on the wind-tunnel measurements, a companion paper (Li *et al*. 2016) explores the boundaries for applying such a model through Computational Fluid Dynamics simulation approaches.

Before continuing the discussion on the twist effect, it is beneficial to illustrate the prevalence of the twist effect in Hong Kong, a metropolitan area surrounded by hilly and complex terrains. Such illustration would demonstrate that the twist effect, which has been commonly ignored in the policy-making for cities with similar situations, could be frequently observed in even highly built-up areas of a metropolis. In a project aiming better air ventilations inside the urban morphology of Hong Kong (Ng 2009), a series of wind-tunnel topographic studies have been conducted in the Wind/Wave Tunnel Facility in the Hong Kong University of Science and Technology. In these studies, urban morphologies, including the surrounding terrain topographies, of selected sites in Hong Kong are scaled-down to the wind tunnel (HKPD 2008a, HKPD 2008b). Since the mean wind speed and direction profiles at the site of interest are measured in the wind-tunnel tests, the prevalence of the twist effect could be illustrated through examining the wind direction difference between the near-surface level ($25\ \mathrm{m}$ in full scale) and the profile top ($500\ \mathrm{m}$ in full scale), which is $0°$ in most cases. Consequently, the wind-tunnel measurements of yaw angles at the near-surface level (θ_{surf}) are used as an indicator to show the prevalence of the twist effect in Hong Kong. Fig. 1 shows the exceedance probability of near-surface yaw angle calculated based on the entire database accumulated in the wind-tunnel topographic studies. It is evident from Fig. 1 that more than 10% of the profiles exhibit a near-surface yaw angle exceeding $15°$. Given the influence of the direction of the approaching wind on the torsional response of high-rise buildings and on the pedestrian level wind field, a difference of $15°$ could be significant. Hence, it is necessary to systematically investigate the direction changes for the purpose of assisting policy making in Hong Kong concerning the pedestrian level wind environment.

Following the introduction, Section 2 presents the detailed description of the wind-tunnel tests and the measurement procedures. Discussions of the yaw angles, and hence on the direction changes, observed in the wind tunnel tests are presented in Section 3. Based on the wind-tunnel measurements, a descriptive model is developed. While the first part of Section 4 mathematically introduces the model, the second part presents a preliminary evaluation of the proposed model.

Concluding remarks are presented in Section 5.

2. Wind-tunnel generic hill test

In order to study the direction changes, a series of wind-tunnel tests were conducted. In these tests, a generic hill model was employed, and the measurements of mean wind speeds and directions at a three-dimensional grid system were utilized to calculate the vertical and horizontal variations of yaw angles.

2.1 Generic hill models with various aspect ratios

Three-dimensional, idealized hill models with various length-to-width aspect ratios were manufactured using the adopted simulation length scale factor of 1:500. The hill models were designed to represent low hills whose height and base length in the longitudinal direction are $100\ \mathrm{m}$ and $1.2\ \mathrm{km}$, respectively (all in full scale). As the geometric scale of the test was $1{:}500$, the hill model was $200\ \mathrm{mm}$ in height and the model base length in the longitudinal direction was $2400\ \mathrm{mm}$. The blockage ratio of all the hill models was about 3.9%, which is less than the critical blockage 5% for topographic wind-tunnel test (Simiu and Scanlan 1996). The elevation of the hill surface can be calculated according to the horizontal location as

$$z = \frac{H}{2} + \frac{H}{2} cos\left(\frac{\pi}{2L_1}\sqrt{x^2 + Ay^2}\right) \tag{2}$$

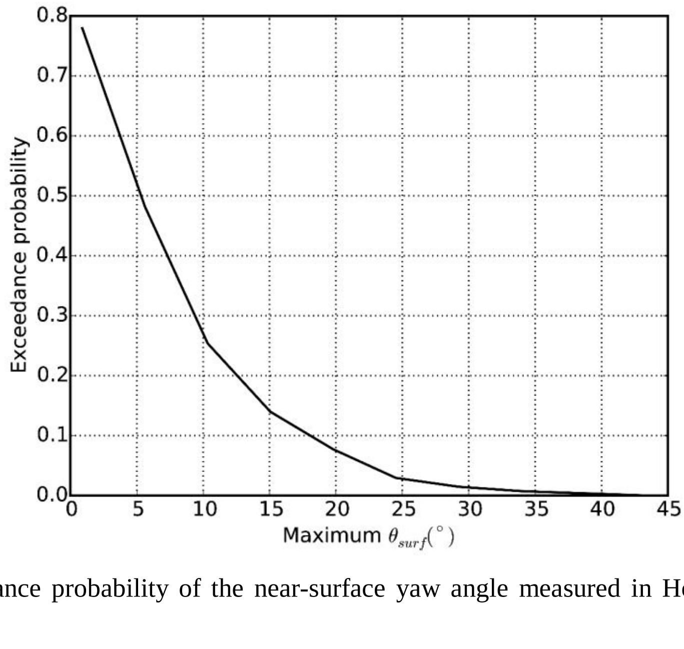

Fig. 1 The exceedance probability of the near-surface yaw angle measured in Hong Kong topographic wind-tunnel studies

where x and y are the horizontal coordinates with the origin located underneath the hill peak, z is the elevation of the hill surface, L_1 and L_2 are the characteristic hill length scales in the longitudinal and lateral directions, respectively, H is the hill peak height and A is the length-to-width aspect ratio of the hill model. The characteristic hill length scale is defined as the horizontal distance travelled by a point moving from the peak to the point where the height is half of the total hill height. The length-to-width aspect ratio is defined as the ratio between characteristic hill length scales in the longitudinal direction and in the lateral direction, i.e., $A = L_1/L_2$. A schematic diagram of a generalized hill model is shown in Fig. 2.

The hill models were manufactured with different length-to-width aspect ratios. In detail, a circular-based hill (i.e., $A = 1$) and two elliptical-based hills (i.e., $A = 2$ and $A = 3$) were manufactured. The maximum hill slope along the primary axis of the hill model is about $15°$ for all the hill models. Thus, non-separated flows are expected when wind flow is parallel to the primary axis of the hill (Lubitz and White 2007). In addition, the hill models with the aspect ratios of 2 and 3 were rotated by an angle of $90°$ to have the primary axis of the hill model lie in the lateral direction to show the influence of flow separations on the twist effect. Equivalently, the rotations provided two more hill models with the aspect ratios of $1/2$ and $1/3$.

All hill models were constructed as "stepped" models to generate the fully turbulent wind flow in the wind-tunnel. In detail, the "stepped" hill models were manufactured using 5 mm thick polystyrene foam sheets. Fig. 3 shows a photo taken in the wind-tunnel where a circular-based stepped hill model was installed. "Stepped" hill models are regularly used to conduct wind-tunnel topographic studies which produced scientifically validated results (Lindley *et al*. 1981, Derickson and Peterka 2004, Lubitz and White 2007). Since localized turbulence is generated from the wind flows passing over steps, there is no need to further roughen the hill model surface to guarantee the Reynolds number independence (Derickson and Peterka 2004). An important parameter in manufacturing a "stepped" hill model is the step size. Large step sizes may induce undesirable local effects in the flow field adjacent to the hill model, which subsequently results in a significant deviation from the wind flow in the real world (Lindley *et al*. 1981).

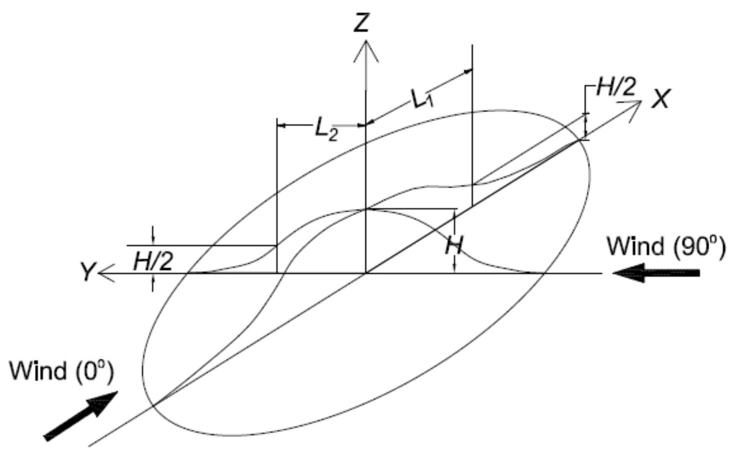

Fig. 2 Schematic diagram of hill models with the coordinate system and definitions of characteristic length scales L_1, L_2 and the hill height

The study by Derickson and Peterka (2004) clearly demonstrated that a proper step size would lead to the wind field perturbed by a "stepped" hill model similar to the wind field perturbed by a "smoothed" hill in full scale. In the present study, a step size of $5\,\mathrm{mm}$ was used, which is equivalent to $2.5\,\mathrm{m}$ in the full scale. Provided that the surface Reynolds number $(u_* z_o/\upsilon)$ is greater than 5, a step size of $5\,\mathrm{mm}$ is considered sufficient to produce an aerodynamically rough flow (Snyder 1972).

2.2 Wind-tunnel test specifications

All wind-tunnel tests were conducted in the Wind/Wave Tunnel Facility of the Hong Kong University of Science and Technology. The wind-tunnel is of the closed circuit type with the maximum wind speed of $25\,\mathrm{m/s}$ allowed in high-speed test section. The high-speed test section, in which the hill models were placed, is $3\,\mathrm{m}$ wide and $2\,\mathrm{m}$ high with a turntable of $2\,\mathrm{m}$ in diameter. There are rows of mechanically controlled roughness blocks installed upstream the turntable. The roughness blocks were controlled to emerge from the floor, to generate the desired approaching mean wind speed and turbulence intensity profiles. If the roughness blocks alone are inadequate to produce the desired profiles, different techniques such as saw-toothed boards and spires are employed.

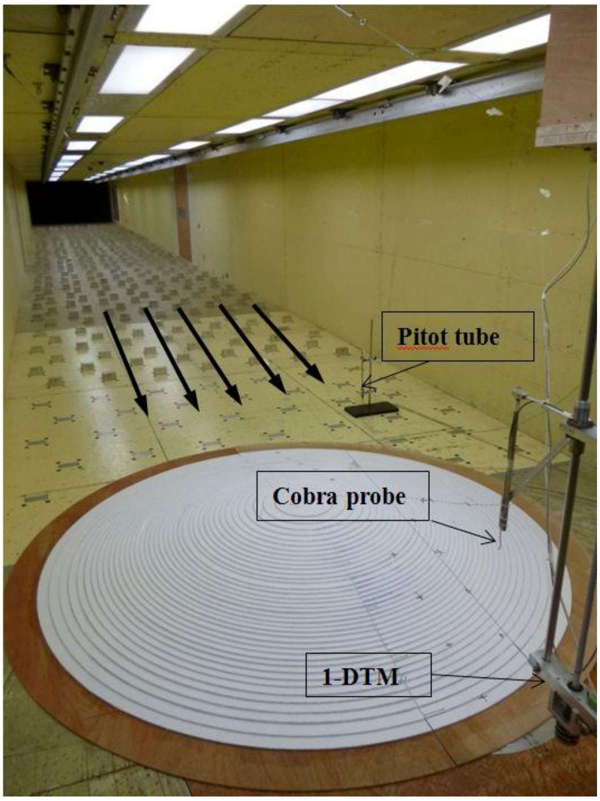

Fig. 3 The wind-tunnel test setup and a generic hill model with an aspect ratio of 1. The approaching wind flow is indicated by the array of arrows

The mean wind profile was calibrated according to the power-law model with the power index of 0.15. The turbulence intensity profile, on the other hand, was calibrated according to the provision given in AS/NZS 1170.2:2002 (Australian/New Zealand Standard 2002) for the open terrain category. The mean wind speed and the turbulence intensity at the hill model height were $5.40\ \mathrm{m/s}$ and 16.9%, respectively. A Cobra probe (TFI® series 100) was used to measure wind speeds and turbulence intensities at a three-dimensional grid system over the generic hill. The Cobra probe, which measures the wind speeds at a frequency of 1000 Hz lasting 65 seconds, was attached to a 1-dimensional (vertical) traverse system, which lifts the Cobra probe to preset heights under the control of a computer. Although the Cobra probe is not suitable for taking measurements in the reversed flow, the geometry of the hill model keeps the reversed flow to a minimum level. If flow separations were observed, such as in the wind-tunnel tests corresponding to the aspect ratios of $1/2$ and $1/3$, the measurements taken near immediately behind the hill are omitted. Previous researchers have employed cobra probes in similar topographical wind-tunnel studies (Ngo and Letchford 2009, McAuliffe and Larose 2012).

The grid, at which the measurements are taken, was defined according to the coordinate system shown in Fig. 2. In the horizontal plane, the x coordinate of the grid increased from -1200 mm to 2000 mm in a step of 200 mm and the y coordinate increased from 0 mm to 1200 mm in a step of 200 mm. In the vertical direction, there were 12 measuring heights corresponding to each horizontal grid point, i.e., $10,\ 20,\ 30,\ 40,\ 50,\ 75,\ 100,\ 150,\ 200,\ 250,\ 300,\ 400$ mm above the local ground. The full set of grid points was only employed in the case where the aspect ratio of the hill model equalled 1. When the aspect ratio equaled 2 and 3, the lateral boundary of the measurement grid was reduced from $y = 1200$ mm to $y = 800$ mm and $y = 400$ mm, respectively. When the aspect ratio equaled $1/2$ and $1/3$ (resulting from the rotation of the hill models with the aspect ratios of 2 and 3 by $90°$), the front boundary was reduced from $x = -1200$ mm to $x = -600$ mm and $x = -400$ mm, respectively.

3. Discussion on the topography-driven twist effect

Based on the wind-tunnel measurements of wind velocity vectors, the vertical profiles of yaw angles at various locations were calculated. The yaw angle near the hill surface (θ_{surf}) is defined as the yaw angle measured at the lowest grid points, i.e., 10 mm in the model scale or 5 m in the full scale, above the local ground. Because the yaw angle reduces to zero at heights beyond the influence of the hill model, θ_{surf} indicates the significance of the twist effect. Contours of θ_{surf}, as shown in Fig. 4, demonstrate that there are two maxima of θ_{surf} in each figure: one at the windward side with positive value (i.e., anti-clockwise) and the other at the leeward side with negative value (i.e., clockwise). Furthermore, Fig. 4 shows that the two maxima of θ_{surf} are found near the line of $y = L_2$. Considering the symmetry of the hill model shown in Fig. 4, the locations of two maxima of θ_{surf} indicate that the twisting effect is most significant at the halfway wrist of a mountain ($x = -1.2L_1$ and $y = L_2$). For hills with various aspect ratios, the locations of the positive-maximum θ_{surf} are summarized in Table 1 and the locations of the negative-maximum θ_{surf} are summarized in Table 2. The results shown in Tables 1 and 2 confirm that the maximum θ_{surf} occurs near the line of $y = L_2$. The coordinates of the absolute maxima, on the other hand, imply that the twist effect has a larger length scale at the leeward side than the windward side, especially for the hill models with aspect ratios less than 1.

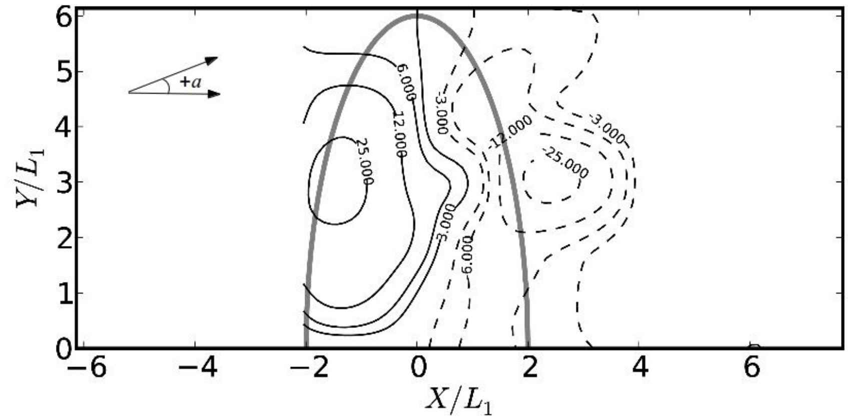

(a) A = 1/3

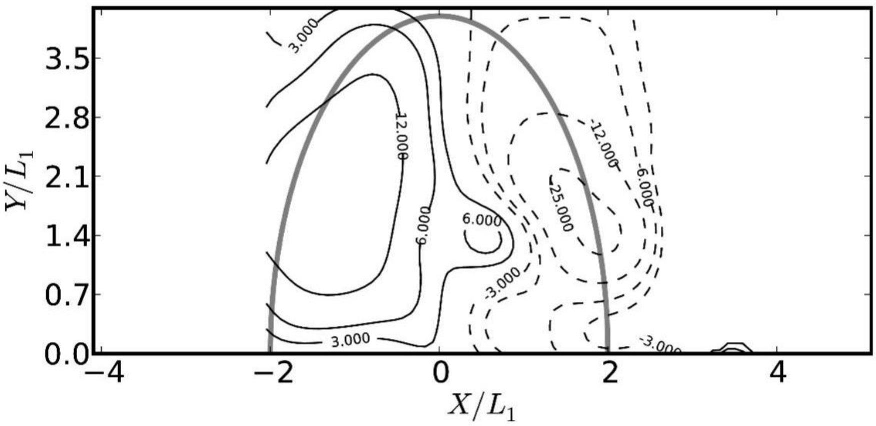

(b) A = 1/2

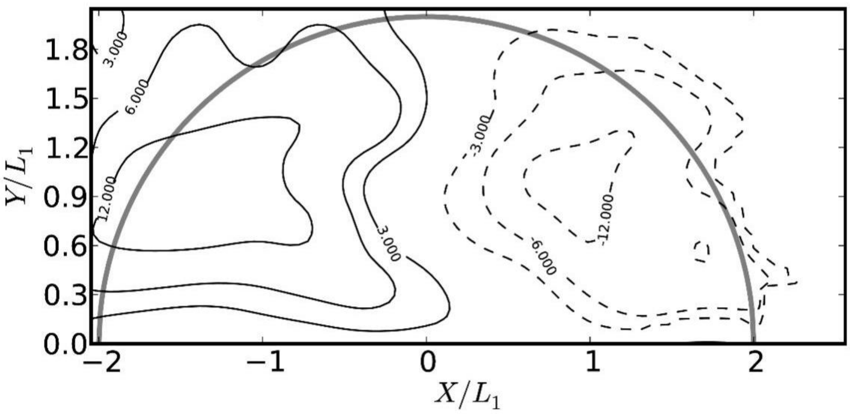

(c) A = 1

Continued-

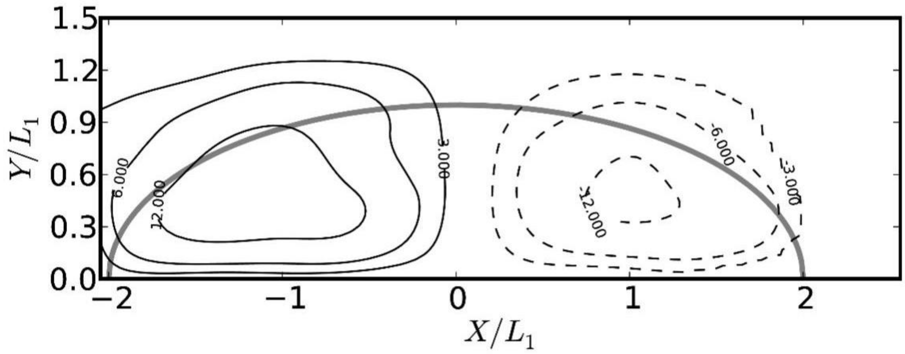

(d) A = 2

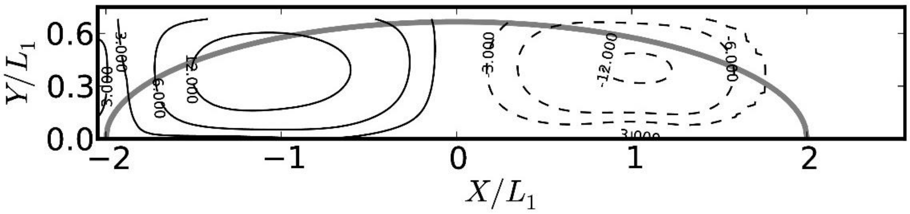

(e) A = 3

Fig. 4 The contours of θ_{surf} measured in the wind-tunnel tests for the hill models with aspect ratios of $1/3$ (a), $1/2$ (b), 1 (c), 2 (d) and 3 (e). The definition of the positive yaw angle is defined in Fig. 4(a)

Table 1 The locations of the positive maximum

Aspect ratio	$^1/_3$	$^1/_2$	1	2	3
X/L_1	-1.4	-1.4	-1.5	-1.2	-1.2
Y/L_2	1.0	1.0	1.0	1.0	1.1

Table 2 The locations of the negative maximum

Aspect ratio	$^1/_3$	$^1/_2$	1	2	3
X/L_1	2.4	1.9	0.8	1.0	1.0
Y/L_2	1.0	1.0	1.0	1.0	1.0

As well as the near-surface yaw angle (θ_{surf}), the twist height (h_θ), which is defined as the height where the absolute value of the yaw angle is less than 3°, shows the height above which the twist effect can be neglected. Fig. 5 presents the contour of the normalized h_θ (divided by the hill height). It is obvious that h_θ varies horizontally, and the difference in h_θ at different locations can be as large as nearly twice the hill height. Apparently, the horizontal variations of h_θ can be resulted from (a) the horizontal variation of θ_{surf} and (b) the difference in the decays of the lateral wind velocities at different positions. When comparing the contours of θ_{surf} and h_θ shown in Figs. 4 and 5, it has been found that both contours have similar patterns. Therefore it can be asserted that the horizontal variations of h_θ are primarily associated with the horizontal variations of θ_{surf} while the vertical decay of the lateral wind velocity v is similar, regardless of the horizontal position.

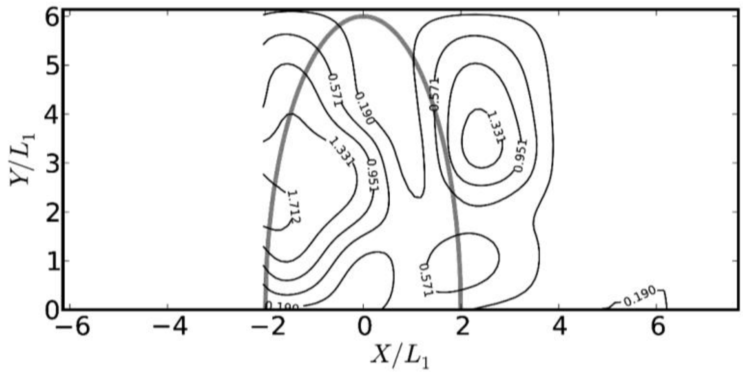

(a) $\mathrm{A} = 1/3$

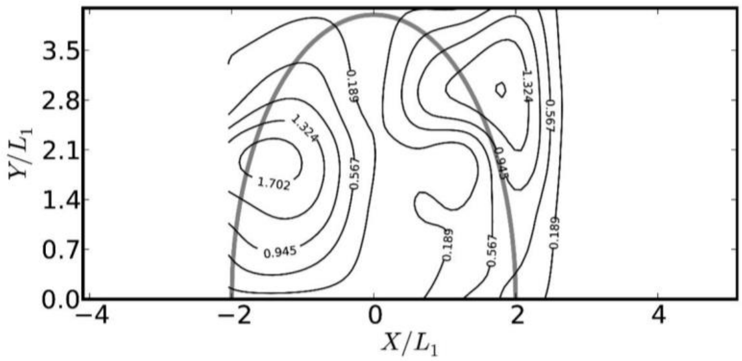

(b) $\mathrm{A} = 1/2$

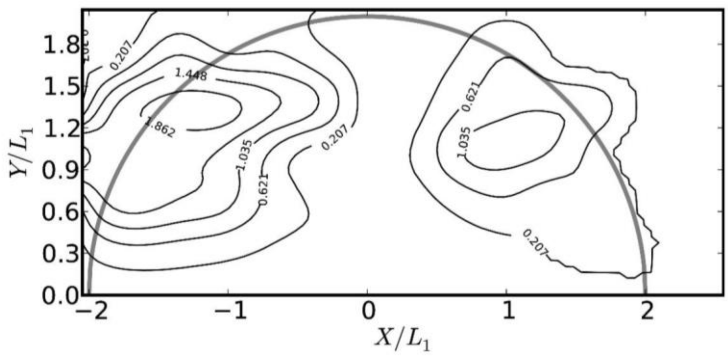

(c) $\mathrm{A} = 1$

Continued-

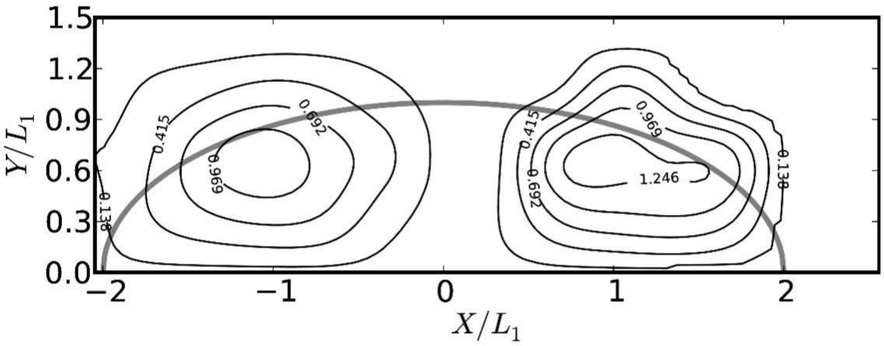

(d) A = 2

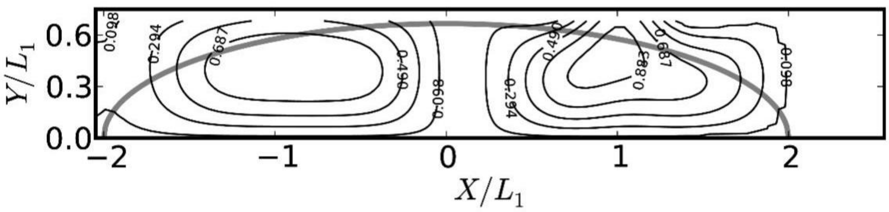

(e) A = 3

Fig. 5 The contours of h_θ measured in the wind-tunnel tests for the hill models with aspect ratios of $1/3$ (a), $1/2$ (b), 1 (c), 2 (d) and 3 (e)

4. A descriptive model

Clearly, it is highly impractical to conduct either a wind-tunnel test or a numerical simulation to predict the direction changes induced by a full range of specific hilly topographies. A descriptive model is therefore necessary to preliminarily estimate the spatial variations of wind directions over hilly terrains. Such a model would take into consideration the main features of the hill geometries, and predict the vertical variations of wind direction at a specific horizontal locations.

By examining the wind-tunnel experimental results, a descriptive model is proposed. The proposed model has two mathematically-separated parts: one calculates the vertical variation of yaw angles and the other predicts the near-surface yaw angle (θ_{surf}) based on the geometry of the hill. Considering that the model describes the vertical and horizontal variations of the direction changes separately, validation has been carried out for the two parts in sequence based on the wind-tunnel measurements. Section 4.1 mathematically presents the proposed model, Sections 4.2 and 4.3 show the validation.

4.1 Formulation of the model

Before introducing the model, it is beneficial to briefly review the only publicly-available engineering model calculating the three-dimensional variations of yaw angles above hilly terrains, the ESDU model. According to the ESDU document (ESDU 1993), the wind direction field above a mountain with known geometries can be calculated in two steps. First, the vertical profile of yaw angles can be calculated as

$$\frac{\theta(h)}{\theta_{surf}} = \frac{1}{1+8.5\frac{h}{H}} \tag{3}$$

In Eq. (3), h is the height above the local ground, θ_{surf} is the yaw angle at the near-surface level, and H is the hill height. It is evident from Eq. (3) that the calculation of the vertical profile of yaw angles takes the yaw angle near surface as an input parameter. In order to estimate the near-surface yaw angle, ESDU model introduced a lateral perturbation parameter and provided a set of formulae to calculate the horizontal variations of near-surface yaw angles given the known geometries of the mountain. In detail, the lateral perturbation parameter is defined as

$$s_v = \frac{K \tan\theta_{surf}}{(dz/dy)_{0,y}} \tag{4}$$

and the horizontal variation of the lateral perturbation parameter is calculated as

$$\begin{cases} \frac{s_v}{s_{vmax}} = \exp\left[-\left(\frac{x}{L_1}+1\right)^2\right] & \frac{x}{L_1} < -1 \\ \frac{s_v}{s_{vmax}} = \sin\left(-\frac{\pi}{2}\frac{x}{L_1}\right) & -1 < \frac{x}{L_1} < 0 \\ \frac{s_v}{-0.8s_{vmax}} = \sin\left(\frac{\pi}{2}\frac{x}{1.2L_1}\right) & 0 < \frac{x}{1.2L_1} < 1 \\ \frac{s_v}{-0.8s_{vmax}} = \exp\left[-\left(\frac{x}{L_1}-1.2\right)^2\right] & \frac{x}{1.2L_1} > 1 \end{cases} \tag{5}$$

$$s_{vmax} = \min\left(\frac{1.83/A}{1+0.84/A}, 1.75\right) \tag{6}$$

In Eq. (4), s_v is the lateral perturbation parameter, K is the speed-up factor calculated according to a speed-up-effect-describing model, z is the surface elevation of the hill surface and $(dz/dy)_{0,y}$ is the local hill slope along the centerline of the hill model in the lateral direction. In Eq. (5), s_{vmax} is the maximum lateral perturbation parameter and L_1 is the characteristic length scale of the hill model in the longitudinal direction. In Eq. (6), A is the aspect ratio of the hill. Consisting Eqs. (3), (5) and (6), the three-dimensional variations of yaw angles above a mountain with known geometries could be calculated.

Following the philosophy adopted by the ESDU model, it is postulated that the decay of the lateral wind component v in the vertical direction is independent from the horizontal location. In other words, once the vertical variation of the lateral wind velocity v is properly normalized, its vertical variation can be described by a universal function regardless of the horizontal location. Because (a) there are various models already available to describe the speed-up effect induced by three-dimensional hills with different geometries and (b) the hill-induced perturbations in the wind direction field is physically related to the perturbations in the wind direction field, it is advantageous if the proposed model relies on the vertical variation of wind speeds to calculate the vertical variation of wind directions.

Through properly normalizing the longitudinal and lateral wind velocities measured in the wind-tunnel experiments, it can be discerned that the vertical variation of v linearly depends on the vertical variation of u. Consequently, it is postulated that

$$v(\mathrm{z}) = c_1 u(\mathrm{z}) + c_2 \quad (7)$$

In Eq. (7), c_1 and c_2 are two parameters defining the vertical variation of the lateral wind velocity v in terms of the vertical variation of the longitudinal wind velocity u.

As in the ESDU model, the concept of the lateral perturbation parameter is adopted. In fact, the lateral wind velocity v calculated according to Eq. (7) at the lowest measurement height (10 mm in the model scale and 5 m in the full scale), which will be termed as critical lateral wind velocity v_c, is chosen to be the indicator equivalent to θ_{surf} in equation(4). As a result, the lateral perturbation parameter in the proposed model is defined as

$$s_v = \frac{v_c/V}{(dz/dy)_{0,y}} \quad (8)$$

Given the definition of the lateral perturbation parameter shown in Eq. (8), Eqs. (5) and (6) can be once again employed to calculate the horizontal variations of the revised lateral perturbation parameter. In Eq. (8), symbols have similar meanings as in Eq. (4) and V is the wind velocity magnitude at the same level as v_c. Considering that Eq. (3) requires two inputs (c_1 and c_2), a single parameter of critical lateral wind velocity is inadequate to support the use of Eq. (3). In the proposed model, another parameter, the critical longitudinal wind u_c is introduced to complement Eqs. (7) and (8). From a theoretical point-of-view, it is clear that the lateral wind velocity in a twisted profile does not change signs, but vanishes as the height increases. If u_c is defined as the longitudinal wind velocity corresponding to zero lateral wind velocity, u_c is related to c_1 and c_2 as

$$u_c = \frac{-c_2}{c_1} \quad (9)$$

In theory, the disappearance of the lateral wind velocity means that the critical longitudinal wind equals to the unperturbed, total wind speed in the approaching wind flow. Consequently, the value of u_c can be, in practice, calculated by averaging the wind speeds in the approaching wind profile at the altitudes higher than three times the hill height. From the definition, it can be seen that u_c is a constant regardless of the horizontal location. Because there are two parameters available to show the horizontal variation of the twist effect in the proposed model (v_c and u_c), Eq. (7) is fully determined. In summary, Eqs. (7), (5), (6) and the definitions of s_v and u_c, v_c constitute a model comprehensively describing the twist effect.

4.2 The vertical variation

Through comparing the yaw angles measured in the wind-tunnel experiment to the model calculations, the proposed model can be evaluated systematically. Since the proposed model describe the vertical and horizontal variations of the twist effect separately, it is logical to evaluate them individually.

Since the evaluation presented in the section focused on the vertical description of the twist effect, it is important to exclude, as much as possible, the influence of the horizontal component of the model. Therefore, the longitudinal and lateral wind velocities measured in the wind-tunnel experiments are directly employed to calculate c_1 and c_2. After c_1 and c_2 are available, the vertical variation of lateral wind velocities were calculated according to Eq. (7) based on the wind-tunnel measurements of longitudinal wind velocities. When the vertical variation of v is available, the vertical profile of yaw angles, which directly show the twist effect, is derived according to Eq. (1). In order to be illustrative, the wind-tunnel measurements taken in the circular-based hill model test were employed to demonstrate the performance of the proposed model in terms of describing the vertical variation of yaw angles. In fact, the measurements of u and v taken along various longitudinal cutting-planes were employed to derive the parameters of c_1 and c_2. Based on the derived c_1 and c_2, the vertical variations of v, and hence the vertical variation of yaw angles, were calculated. Fig. 6 presents the comparison between the wind-tunnel measured and the model calculated yaw angles, which reveals that the proposed model accurately describes the vertical variations of yaw angles above the circular-based idealized hill. It should be pointed out that the proposed model is not only applicable when the twist effect is prominent, such as along the cutting-planes of $y = 0.68L_1$, but also accurately shows the vertical variation of small-valued yaw angels, such as along the cutting-plane of $y = 0$.

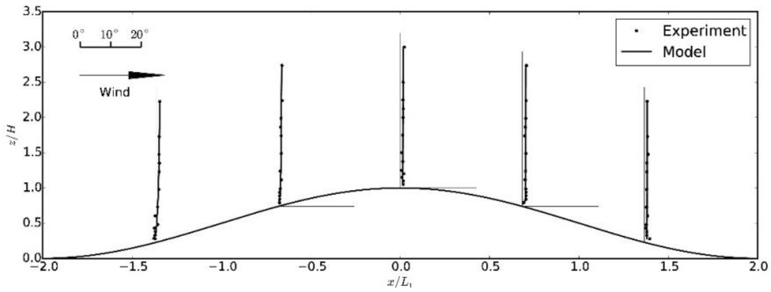

(a) $Y = 0$

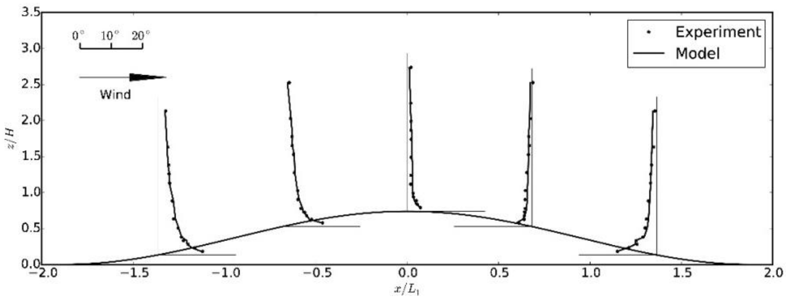

(b) $Y = 0.68L_1$

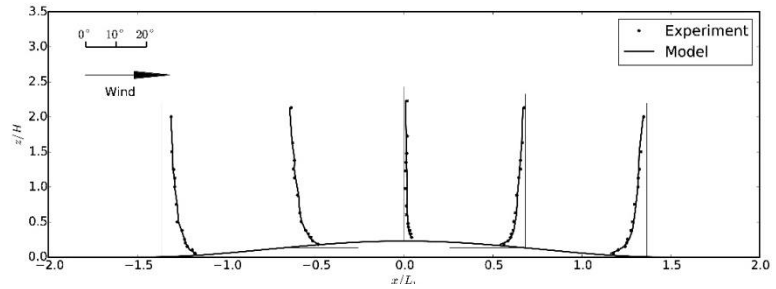

(c) $Y = 1.37L_1$

Fig. 6 The vertical profiles of yaw angles measured along longitudinal cut-planes in the wind-tunnel test of the circular-based hill model

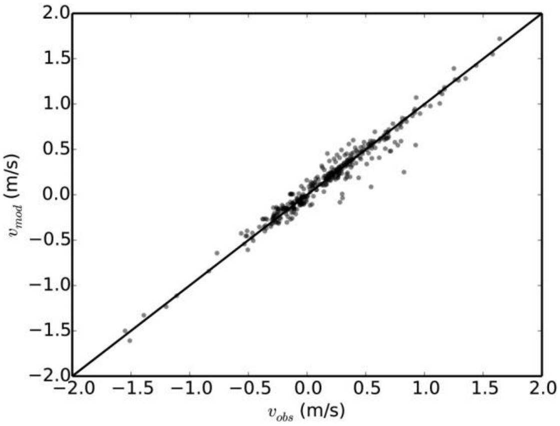

(a)

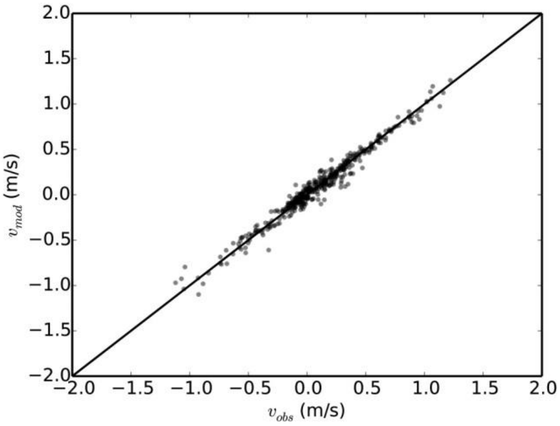

(b)

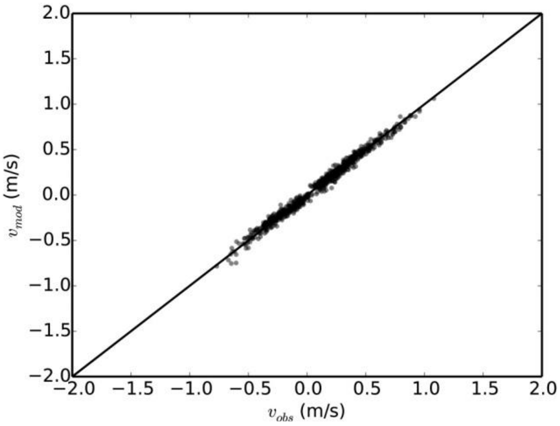

(c)

Continued-

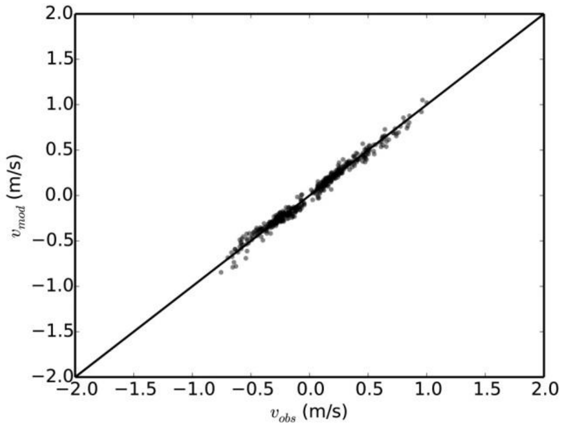

(d)

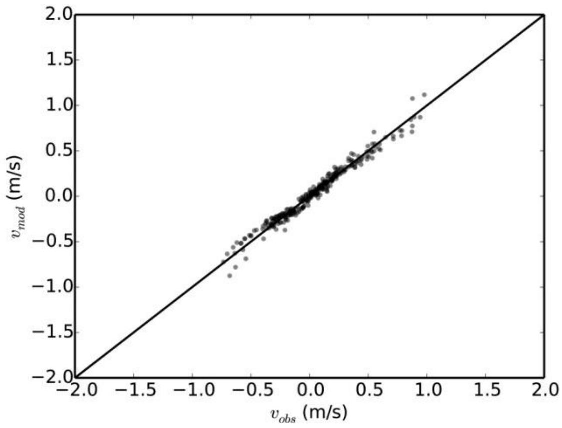

(e)

Fig. 7 The comparisons between lateral wind components measured in the wind-tunnel tests (v_{obs}) and calculated according to Eq. (7) (v_{mod}). The measurements are taken from the wind-tunnel tests of hill models with aspect ratios of $1/3$ (a), $1/2$ (b), 1 (c), 2 (d) and 3 (e)

As regards the quantitative evaluations, the wind-tunnel measured v are compared with the model calculated v for all the hill models. Fig. 7 presents the comparisons corresponding to various hill models. The diagonal lines indicate that the wind-tunnel measured v exactly equals the model calculations. It is clear that the proposed model, or Eq. (7) to be more specific, is adequate to describe the vertical variation of lateral wind velocities regardless of the hill geometry. Even for the hill models with the aspect ratio less than 1, the model calculated v is still close to the values measured in the wind-tunnel experiments. Such agreement indicates that non-separated flow is not a precondition to make Eq. (7) valid.

4.3 Variation in the horizontal plane

From the description of the proposed model (Section 4.1), it is clear that the lateral perturbation parameter is the key parameter in the proposed model. On one hand, the horizontal variation of the lateral perturbation parameter could be calculated through Eq. (5). On the other hand, the wind-tunnel measured u and v could be employed to calculate the lateral perturbation parameter. Given the measured and calculated lateral perturbation parameter, the accuracy and the reliability of Eq. (5) can be quantitatively assessed. In order to make this clearer, the lateral perturbation parameters and the x coordinates were normalized before the comparison as

$$s_v{}^r = \begin{cases} \frac{s_v}{s_{vmax}} & x < 0 \\ \frac{s_v}{0.8 s_{vmax}} & x > 0 \end{cases} \tag{10}$$

$$x^r = \begin{cases} \frac{x}{L_1} & x < 0 \\ \frac{x}{1.2 L_1} & x > 0 \end{cases} \tag{11}$$

In Eqs, (10) and (11), $s_v{}^r$and x^r are the normalized lateral perturbation parameter and the normalized coordinate, s_{vmax} denotes the maximum lateral perturbation parameter and L_1 is the characteristic length scale of the hill model along the primary axis.

Fig. 8 shows the variations of $s_v{}^r$, calculated based on the wind-tunnel measurements taken in the circular-based hill test, with x^r. The theoretical curve calculated according to Eq. (5) is also included. From Fig. 8, it is evident that Eq. (5) calculates the horizontal variations of the model parameters with an acceptable accuracy. Nonetheless, systematic deviations are still observed. For example, the scattered points corresponding to the longitudinal cutting-plane of $y = 0$ varies more rapidly than the theoretical curve from positive values to negative values when x^r varies within the range of $(-1,1)$. Moreover, the values of $v_c{}^r$ corresponding to the cutting-plane $y = 0$ in the wake ($x^r > 1.5$) deviate from the predictions made according to Eq. (5). Such observations imply that the definition of the lateral perturbation parameter could be adjusted to better reduce the horizontal variation of lateral perturbation parameter into a function of the normalized coordinate. In other words, although the wind-tunnel experiments show that the proposed model is acceptable to describe the horizontal variation of the twist effect induced by a three-dimensional hill, there is still room for the model to be improved, in terms of both the definition of the lateral perturbation parameter and the function describing the longitudinal variation of the lateral perturbation parameter.

In addition to $v_c{}^r$, the proposed model employs the critical longitudinal wind velocity (u_c) to calculate c_1 and c_2. Theoretically, u_c is a constant in the horizontal plane and equals the approaching wind speed at heights beyond the influence of the hilly terrain. Practically, u_c can be approximated by the upper-level mean wind speed (u_{up}) calculated by averaging the approaching wind speeds above $3H$, where H is the height of the hill. In order to show the validity of this theoretical consideration, the ratio u_c and u_{up} is shown by means of the contours in Fig. 9. It is clear from Fig. 9 that it is valid to approximate u_c by u_{up} in a considerably large region of the wind field perturbed by a three dimensional circular-based hill. More specifically, Fig. 9 shows that the ratio between u_c and u_{up} only deviates from unity in the regions where the mean yaw angle is small. Fig. 10 illustrates the variation of the ratio (u_c/u_{up}) with the absolute value of the mean yaw angle measured in the circular-based hill test. The mean yaw angle was calculated by averaging the absolute values of the measured yaw angles at all the measurement heights. It is evident from Fig. 10 that the ratio approaches unity as the mean yaw angle increases, and the ratio falls into the range of $0.85 \sim 1.15$ when the absolute value of the mean yaw angle exceeds $4°$.

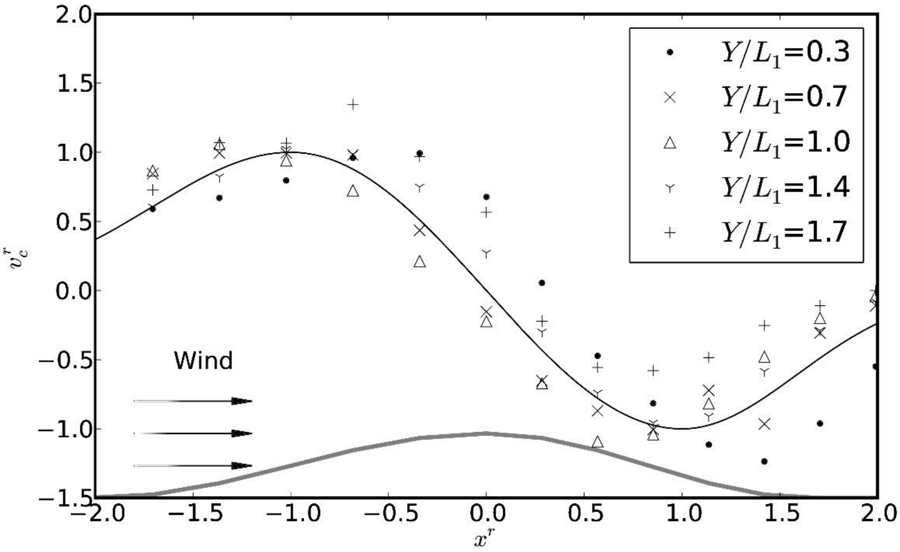

Fig. 8 The variation of v_c^r in the along-wind direction and the curves calculated according to equation (5) (solid line). The calculations were based on the wind-tunnel results of a circular-based hill model $(A = 1)$

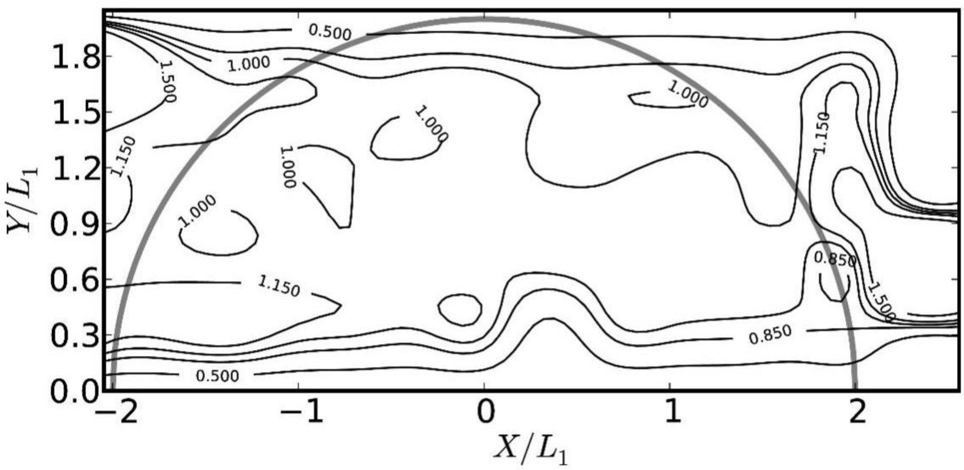

Fig. 9 The contours of the ratio between u_c and u_{up} corresponding to the wind-tunnel test of the circular-based hill model

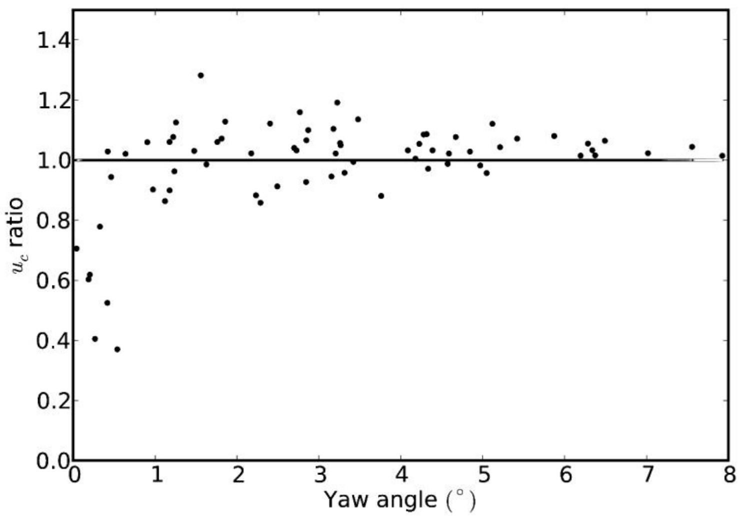

Fig. 10 The variation of the ratio between u_c and u_{up} with the mean yaw angle, calculated based on the measurements taken in the circular-based hill model wind-tunnel test

Similar to Fig. 9, the longitudinal variations of the normalized lateral perturbation parameters calculated based on the wind-tunnel measurements taken in the experiments corresponding to different aspect ratios are presented. Fig. 11(a) shows the longitudinal variation of ${s_v}^r$ corresponding to the hill model with the aspect ratio of 2 and Fig. 11(b) shows the variation corresponding to the aspect ratio of $1/2$. Since the wind-tunnel test results corresponding to aspect ratios of 3 and $1/3$ are similar to those corresponding to aspect ratios of 3 and $1/3$, their figures are omitted. From Fig. 10, it can be concluded that Eq. (5) is valid to describe the horizontal variation of the twist effect when the primary axis of the hill appears in the longitudinal/along-wind direction. From Fig. 11, it is clear that Eq. (5) is inadequate to describe the horizontal variation of the lateral perturbation parameter when the primary axis of the hill appears in the lateral direction, especially in the wake zone. Therefore, further improvements are required for the proposed model to reliably describe the horizontal variation of the twist effect when the aspect ratio of the hill is less than 1. Since the flow separation was observed in the wind-tunnel experiments of the hill models with aspect ratios of $1/2$ and $1/3$, it is argued that flow separation is the reason for the deviations observed in Fig. 11(b), and therefore the improvement of the twist-effect-describing models could be based on better understanding of the wind direction variations in the separated flows.

Eq. (5) alone is insufficient to calculate the horizontal variation of the lateral perturbation parameter (s_v) because of the undetermined maximum lateral wind perturbation parameter (s_{vmax}). The evaluation of Eq. (6) to predict s_{vmax} should, however, rely on a larger database containing the wind direction fields perturbed by differently-shaped hills. Consequently, the validity of Eq. (6), which is extracted from the ESDU model, remains a topic for future studies.

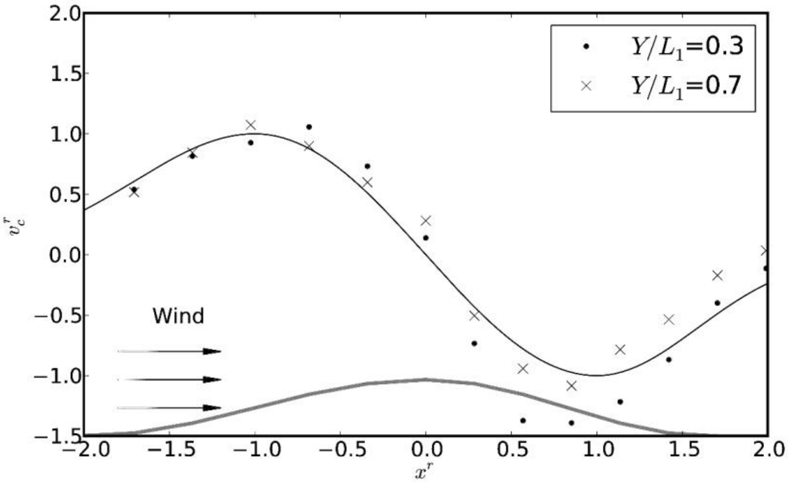

(a)

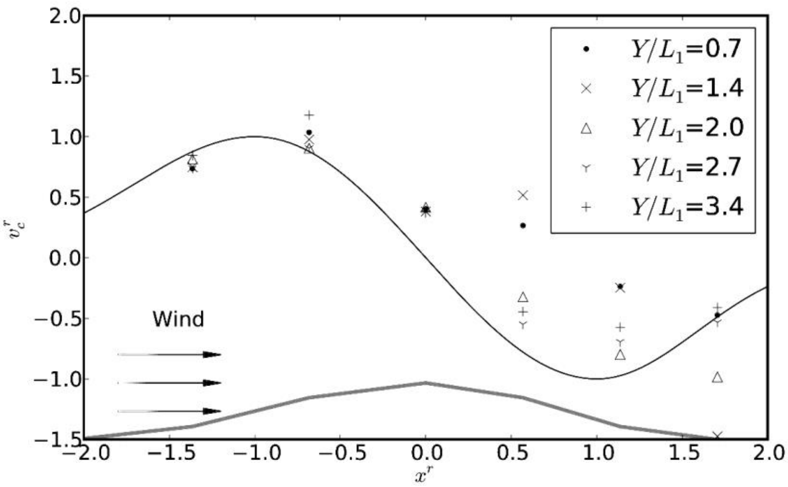

(b)

Fig. 11 The variation of $v_c{}^r$ in the longitudinal direction and the curves calculated according to equation (5) (solid line). The calculations were based on the wind-tunnel results of a hill model with an aspect ratio of 2 (a) and $1/2$ (b)

5. Conclusions

The direction changes induced by hilly topographies are important when assessing wind loads on structures, predicting air pollutants dispersion processes and investigating the wind energy resources in a mountainous area. Although a number of previous studies have been conducted to investigate the influence of the hill topography on the wind speed field above the hill surface (i.e., the speed-up effect), the twisting effect induced by the hilly topography has not been studied as thoroughly as the speed-up effect. In fact, to the best of our knowledge, the ESDU model is the only model, describing direction changes, available to the public for engineering applications. The ESDU model, however, has not yet been scientifically validated using either field measurements or wind-tunnel test results.

The direction changes induced by a three-dimensional hill was investigated by testing several generic hill models with different aspect ratios in a boundary layer wind-tunnel. From the wind-tunnel test results, it has been found that,

- the twist effect was most obvious near halfway wrist of the mountain, and the twist effect at the windward side is more significant than at the leeward side;
- the characteristic height scale of the wind field perturbed by a three-dimensional hill varies significantly, in accordance with the variation of the near-surface yaw angle;
- the characteristic length scale in the wind field perturbed by a three-dimensional hill is larger in the wake;

Acknowledgements

The work described in this paper was supported by the Research Grants Council of the Hong Kong Special Administrative Region, China (Project No. 9041338 and DAG11EG06), the Economy, trade and Information Commission of Shenzhen Municipality (Project No. 201510150880 and SZHY2014-B01-001). The authors also gratefully acknowledge the assistance provided by the technical and professional staff of CLP Power Wind/Wave Tunnel Facility at the Hong Kong University of Science and Technology in the conduct of the wind-tunnel experiments reported in this paper.

References

Australian/New Zealand Standard, Structural design actions Part 2: Wind actions, AS/NZS 1170.2:2002.

Derickson, R. and Peterka, J.A. (2004), "Development of a powerful hybrid tool for evaluating wind power inComplex Terrain: Atmospheric numerical models and wind-tunnels", *Proceedings of the 23rd ASME Wind Energy Symposium*, Reno, Nevada,

Engineering Science Data Unit (1993), *Mean wind speeds over hills and other topography, Section No. 91043*, London: IHS ESDU.

Flay, R.G. (1996), "A twisted flow wind-tunnel for testing yacht sails", *J. Wind Eng. Ind. Aerod*., **63**(1), 171-182.

Gong, W. and Ibbetson, A. (1989), "A wind-tunnel study of turbulent flow over model hills", *Bound. - Lay. Metrol*., **49**(1-2), 113-148.

Hedges, K.L., Richards, P.J. and Mallinson, G.D. (1996), "Computer modelling of downwind sails", *J. Wind Eng. Ind. Aerod*., **63**(1), 95-110.

Hong Kong Planning Department (2008a), *Urban Climatic Map and Standards for Wind Environment – Feasibility Study, Working Paper 2B: Wind Tunnel Benchmarking Studies, Batch I*, Hong Kong: the government of Hong Kong special administrative region.

Hong Kong Planning Department (2008b), U*rban Climatic Map and Standards for Wind Environment – Feasibility Study, Working Paper 2C: Wind Tunnel Benchmarking Studies, Batch II*, Hong Kong: the government of Hong Kong special administrative region.

Jackson, P.S. and Hunt, J.C.R. (1975), "Turbulent wind flow over a low hill", *Q. J. Roy. Meteorol. Soc*., **101**(430), 929-955.

Jazcilevich, A.D., García, A.R. and Caetano, E. (2005), "Locally induced surface air confluence by complex terrain and its effects on air pollution in the valley of Mexico", *Atmos. Environ*., **39**(30), 5481-5489.
Li, S.W., Hu, Z.Z., Tse, K.T. and Weerasuriya, A.U. (2016), "Wind direction field under the influence of topography. II. CFD investigations", *Wind Struct*., submitted.
Lindley, D., Neal, D., Pearse, J. and Stevenson, D. (1981), "The effect of terrain and construction method on the flow over complex terrain models in a simulated atmospheric boundary layer", *Proceeding of the 3rd British Wind Energy Association Wind Energy Conference*, Cranfield, UK.
Lubitz, W.D. and White, B.R. (2007), "Wind-tunnel and field investigation of the effect of local wind direction on speed-up over hills", *J. Wind Eng. Ind. Aerod*., **95**(8), 639-661.
Mason, P.J. and Sykes, R.I. (1979), "Flow over an isolated hill of moderate slope", *Q. J. Roy. Meteorol. Soc*., **105**(444), 383-395.
McAuliffe, B.R. and Larose, G.L. (2012), "Reynolds-number and surface-modeling sensitivities for experimental simulation of flow over complex topography", *J. Wind Eng. Ind. Aerod*., **104**, 603-613.
Ngo, T. and Letchford, C. (2009), "Experimental study of topographic effects on gust wind speed", *J. Wind Eng. Ind. Aerod*., **97**, 426-438.
Palma, J.M.L.M., Castro, F.A., Ribeiro, L.F., Rodrigues, A.H. and Pinto, A.P. (2008), "Linear and nonlinear models in wind resource assessment and wind turbine micro-siting in complex terrain", *J. Wind Eng. Ind. Aerod*., **96**(12), 2308-2326.
Simiu, E. and Scanlan, R.H. (1996), *Wind effects on structures*, John Wiley & Sons.
Snyder, W. (1973), "Similarity criteria for the application of fluid models to the study of air pollution meteorology", *Bound. – Lay. Meteorol*., **3**, 113-134.
Taylor, P.A. and Lee, R.J. (1984), "Simple guidelines for estimating wind speed variations due to small scale topographic features", *Climatol. Bull*., **18**(2), 3-32.
Taylor, P.A., Walmsley, J.L. and Salmon, J.R. (1983), "A simple model of neutrally stratified boundary-layer flow over real terrain incorporating wavenumber-dependent scaling", *Bound. – Lay. Meteorol*., **26**(2), 169-189.

JH